Ocean Dynamics (2015) 65:919–930
DOI 10.1007/s10236-015-0848-4

The effect of wind on long-term summer water temperature trends in Tokyo Bay, Japan

Li-Feng Lu[1] · **Ryo Onishi**[1] · **Keiko Takahashi**[1]

Received: 22 October 2014 / Accepted: 3 May 2015 / Published online: 16 May 2015

Abstract The effect of wind on summer water temperature trends in a semi-closed bay (Tokyo Bay, Japan) is examined through several numerical experiments using a high-resolution three-dimensional ocean model. The model is executed under no-wind and uniform southerly/northerly wind conditions, and monthly mean currents and temperature distributions and heat transport in Tokyo Bay for July are calculated. The model results show that wind has a significant effect on heat transport and temperature distribution in the bay. (1) When a southerly wind prevails northward cool water transport intensifies while southward warm water transport declines, thus decreasing the water temperature in the central bay area while increasing temperature at the bay head. (2) A northerly wind has an opposing effect and decreases the water temperature in coastal bay head area while increase the temperature along the southwest coast. The results also suggest that the trend of increasing southerly wind amplitude may have affected water temperature trends in Tokyo Bay from 1979 to 1997. The model results demonstrated that the an intensified southerly wind lowers water temperatures in most areas of the bay by enhancing upwelling and open ocean-water intrusion near the bay mouth while increases temperatures in the bottom layer of the bay head by suppressing southward warm water transport.

Keywords Water temperature trends · Wind · Tokyo Bay · Heat transport

Responsible Editor: Leo Oey

This article is part of the Topical Collection on the *6th International Workshop on Modeling the Ocean (IWMO) in Halifax, Nova Scotia, Canada 23-27 June 2014*

✉ Li-Feng Lu
lifeng_lu@jamstec.go.jp

[1] Center for Earth Information Science and Technology, Japan Agency for Marine-Earth Science and Technology, Yokohama, Kanagawa 236-0001, Japan

1 Introduction

Trends of increasing coastal water temperature with significant impacts on local ecosystems have been recently reported (e.g., Nixon et al 2004; Presten 2004; Shearman and Lentz 2010). However, in Tokyo Bay, a semi-closed bay located along the east coast of Japan (Fig. 1), water temperatures exhibited a descending trend in the surface layer and deep region of the bottom layer in July from 1976 to 1997 (Figs. 3 and 4 in Ando et al. 2003). Similar trends have been observed in Fukuoka Bay, another semi-closed bay in Japan (Aoki and Isobe 2006). The continuation of this decreasing summer water temperature trend will greatly impact not only the local environment and ecosystem but also the coastal urban climate (Oda and Kanda 2009). Therefore, the identification of mechanisms underlying these trends, particularly for the summer season, is ecologically and environmentally important.

The previous studies have suggested that descending summer water temperature trends in these coastal bays are associated with increased cool water intrusion from the open ocean. Yagi et al. (2004) found a negative correlation between long-term summer surface temperature trends and salinity near the bay mouth in Tokyo Bay. Nomura (1996) observed that the number of certain species of zooplankton that reproduce in the outer bay increased in the central bay from 1981 to 1990. To explore the causes of the increased ocean water intrusion, Yanagi (2008) simulated the residual flows for August in

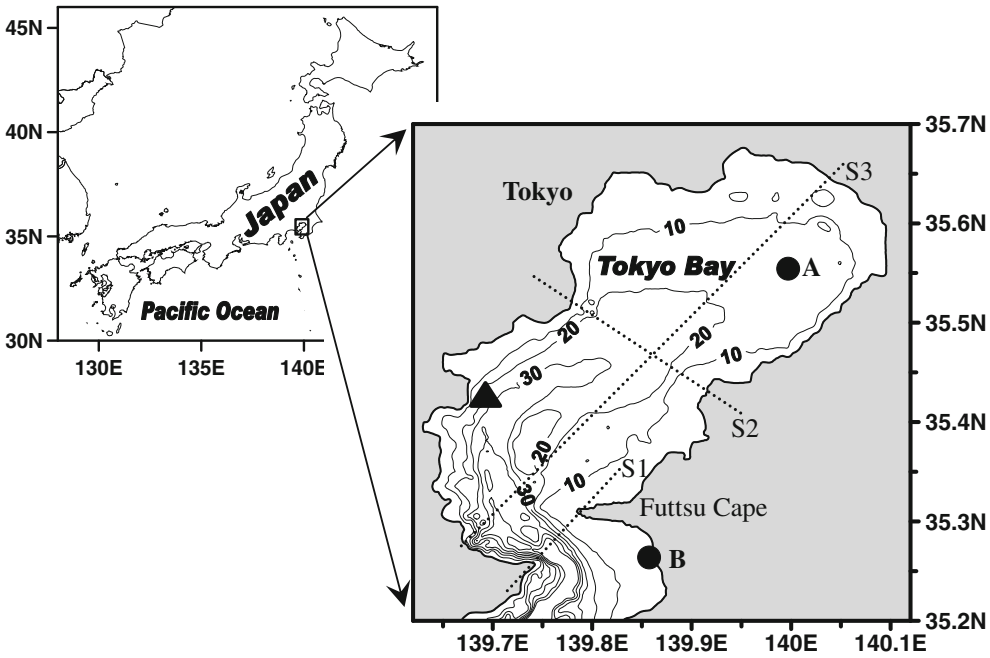

Fig. 1 The study area location and the topography of Tokyo Bay. *Solid lines* denote topographic contours, and *dotted lines* demarcate sections S1, S2 and S3. The *black triangle* denotes the wind observation station, and *black circles* denote the surface water temperature observation stations

Tokyo Bay using a three-dimensional prognostic numerical model. The model results indicated that water exchange between the bay and open ocean was enhanced by intensified gravitational circulation at the bay mouth induced by increased river discharge and decreased tidal amplitude due to reclamation.

However, the mechanisms behind some processes remain unclear. For example, near the bay mouth, there is a negative correlation between water temperature and salinity, suggesting that intrusion by cool ocean water is a major cooling factor, although not for the bay head. Moreover, bay head water temperatures exhibit opposing trends in the surface and bottom layers. To further elucidate the mechanisms that control water temperature trends in Tokyo Bay during strong summer stratification periods, the detailed heat transport pathways in the bay and their dominant processes must be identified.

The heat content in Tokyo Bay is mainly dominated by advective heat transfer related to residual currents (Hinata et al. 2001). Observations and modeling have demonstrated that the residual currents in Tokyo Bay are characterized by strong cyclonic and weak anti-cyclonic circulation at the bay head and bay center, respectively; these circulations are strongly influenced by wind forcing (Unoki et al. 1980; Guo and Yanagi 1996). When southerly/northerly winds prevail, upwelling occurs along the southwest/east coast, inducing internal Kelvin waves propagating cyclonically along the coast (Suzuki and Matsuyama 2000); consequently, bay head water temperatures increase/decrease (Tabeta and Fujino 1996; Hinata et al. 2001). Magome et al. (2012)'s observation and modeling results demonstrated that southerly winds suppress water exchange processes at the bay mouth and trap bay water in the head region. Nakayama et al. (2014) suggested that linear/nonlinear Ekman layers induced by wind curl produce anti-cyclonic/cyclonic circulation immediately below the surface mixed layer, producing material transport convergence/divergence in the bay head region. In addition, wind forcing has considerable effects on the water temperature structure and heat transport processes in other bays, including Fukuoka Bay (Aoki and Isobe 2006) and the Gulf of Mexico (Chang and Oey 2010).

However, few studies have examined the effect of wind on long-term heat transport and water temperature trends in Tokyo Bay. In this study, we use a high-resolution three-dimensional ocean model to examine how wind forcing affects Tokyo Bay heat transport and water temperature trends during the summer.

The paper is organized as follows. The model and its qualitative verification regime are described in section 2. In section 3, the effects of southerly/northerly wind on heat transport are presented. Section 4 discusses the effect of wind on long-term summer water temperature trends in Tokyo Bay and section 5 presents the conclusions.

2 Model description and implementation

2.1 Model description

The Multi-Scale Simulator for the Geoenvironment (MSSG) model is employed in this study. The model is based on incompressible Navier–Stokes equations with the Boussinesq approximation and is designed for parallel computers (Marshall et al. 1997a, b). In a rectangular coordinate system, the

following equations govern the evolution of currents, temperature, salinity, and pressure fields (Marshall et al. 1997a, b).

Motion equation

$$\frac{\partial u}{\partial t} = G_{\mathrm{u}} - \frac{\partial p}{\partial x} \tag{1}$$

$$\frac{\partial v}{\partial t} = G_{\mathrm{v}} - \frac{\partial p}{\partial y} \tag{2}$$

$$\frac{\partial w}{\partial t} = G_{\mathrm{w}} - \frac{\partial p}{\partial z} \tag{3}$$

Continuity equation

$$\frac{\partial u}{\partial x} + \frac{\partial v}{\partial y} + \frac{\partial w}{\partial z} = 0 \tag{4}$$

Temperature and salt equation

$$\frac{\partial T}{\partial t} = G_T, \quad \frac{\partial S}{\partial t} = G_S \tag{5}$$

State equation

$$\rho = \rho(T,\ S,\ p) \tag{6}$$

in which u, v, and w are velocity in the zonal, meridional, and vertical directions, respectively; p denotes the pressure; G_{u}, G_{v}, G_{w} are inertial, Coriolis, metric, gravitational, and forcing/dissipation terms in the zonal, meridional, and vertical directions, respectively; T, S, and ρ represent temperature, salinity, and density, respectively; and G_T and G_S denote advection and diffusion terms for temperature and salinity, respectively.

The finite-volume method is adopted to discretize the model in space, and the Leap-frog scheme with a Robert-Asselin time filter is used for time integration. Horizontal viscosity is calculated using a Smagorinsky-type formulation (Smagorinsky 1963). The vertical mixing process is parameterized using Mellor-Yamada's turbulence kinetic sub-model (Mellor and Yamada 1982). To reduce calculation costs, the surface elevation is solved implicitly.

The computational domain is divided into a 200×200 m horizontal mesh with 30 levels in the vertical z coordinate over a resolution of 1 m near the surface and 2 m near the bottom.

At the southern lateral open boundary, measurements of the monthly mean temperature and salinity derived from the World Ocean Atlas (WOA) (Antonov et al. 2010; Locarnini et al. 2010) are applied. At the surface, the heat flux field calculated from the monthly mean National Centers for Environmental Prediction/National Center for Atmospheric Research (NCEP/NCAR) reanalysis data (Kalnay et al. 1996) is imposed. The COARE 3.0 algorithm proposed by Fairall et al. (2003) is used to compute bulk air-sea fluxes with daily variations in shortwave radiation.

The initial currents are at rest, and the temperature and salinity fields are uniform based on the WOA estimation.

To spin up the model, all calculations were started from January without wind forcing until the currents reached a quasi-equilibrium state and the temperatures reached a steady stratified structure.

2.2 Model validation

To validate the model, monthly mean wind forcing was applied after 1 year spin-up, and calculation was continued for another year. As the present model is driven by climatologically monthly mean forcing, it is impossible to compare modeling results with field observations or other modeling outputs for a specific period. Consequently, a qualitative verification of general modeled features is presented here.

Figure 2 shows the mean circulation and water-temperature distribution in the surface layer (a) and 1 m above the bottom (b) during the summer (from June to August). The model results demonstrate that the Tokyo Bay summer circulation is characterized by anticlockwise circulation at the bay head area and clockwise circulation behind Futtsu cape in the central bay. The model effectively reproduces observed (Unoki et al. 1980) and modeled (Guo and Yanagi 1996) seasonal

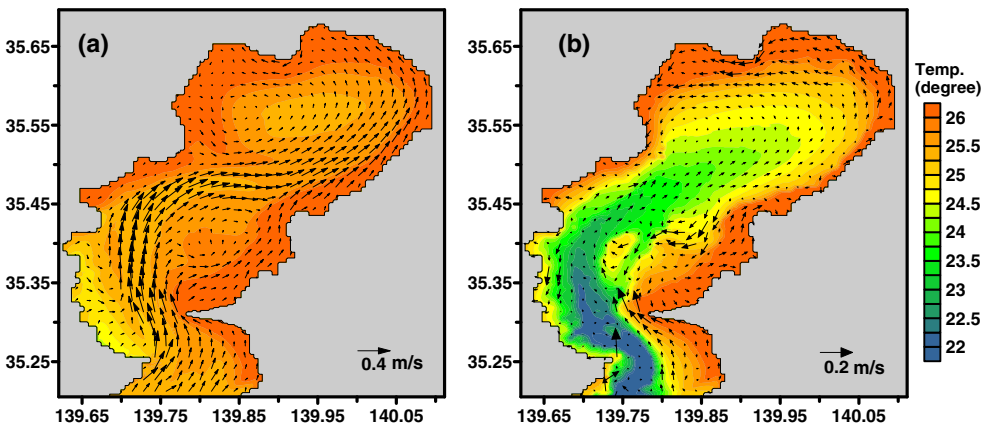

Fig. 2 The mean circulation and water temperature distributions in the surface layer (**a**) and 1 m above the bottom layer (**b**) during the summer (from June to August)

circulation variations characteristics in Tokyo Bay (the results for spring, fall, and winter are not shown).

Figure 3 presents time serials of simulated surface water temperature (red line) and 10-year averaged observations from 2003 to 2013 (black line) at station A (thick lines) and station B (thin lines). The observations indicate that (1) during the warming period (from March to August), the water temperature at the bay head increases faster and exceeds that at the bay mouth. In August, the water temperatures reach a maximum value. (2) During the cooling period (from September to February), the bay head water temperature decreases faster than that at the bay mouth. In February, both temperatures reach a minimum value. The modeling results overestimate the temperatures from August to October and underestimate the temperatures for February but still roughly reproduce general warming and cooling processes.

Overall, the present model effectively reproduces the monthly variations in Tokyo Bay circulation and water temperature.

3 Effects of wind on the heat transport in Tokyo Bay

To examine the effects of wind on the circulation and consequent heat-transport processes in Tokyo Bay, the model was applied without wind forcing and with 3 m/s southerly/northerly winds after an 18-month spin-up period. Then, the calculation was continued for 1 month from July, and all results were averaged over 1 month. Figures 4, 5, 6, 7, 8, 9, 10, 11, 12, and 13 below correspond to the monthly mean results for July.

3.1 No-wind experiment

The upper panel of Fig. 4 shows the monthly mean currents (vectors) and water temperature (shaded) for the surface (left) and bottom (right) layers, respectively, for the no-wind experiment. When no wind is present due to the topographic heat effect (Onishi 1975), the water temperature in the shallow coastal region is higher than that in the deep bay center. Currents are then driven by density differences between warm, shallow water and cool, deep water and between fresh bay water and salty open-ocean water. In the surface layer, cool open-ocean water enters the bay from the western bay mouth, propagates northward to the central bay area, and then moves to the eastern coast, generating a clockwise circulation in the central bay area and two anticlockwise circulations at the bay head and along the southwest coast. At the center of the clockwise/anticlockwise circulations, warm-water pool forms in the central bay area and cool-water pools form at the bay head and along the southwest coast (Fig. 4a). In the bottom layer, anticlockwise circulation in the bay head and clockwise circulation in the central bay area are still evident, and the distribution of water temperature is mainly related to the topographical characteristics (Fig. 4b).

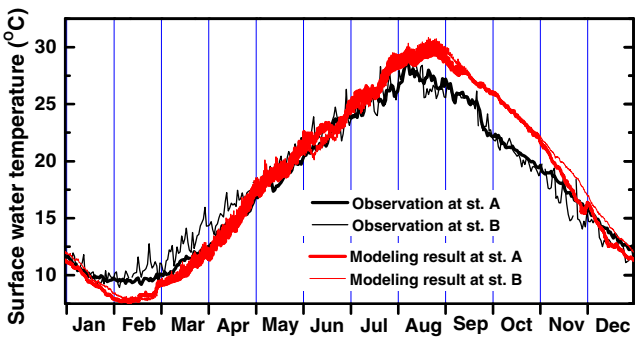

Fig. 3 Time serials of simulated surface water temperature (*red lines*) and 10-year averaged observations for 2003 to 2013 (*black lines*) at stations A (*thick lines*) and B (*thin lines*)

The lower panel of Fig. 4 presents the monthly mean heat transport for the surface (left) and bottom (right) layers. In the surface layer, there is northward cool-water transport at the bay mouth; this transport is strongest after passing the Futtsu Cape due to the narrowed topography and counterflows from anti-clockwise circulation along the southwest coast (Fig. 4a, c). In the central bay area, the strong eastward head transport moves the cool water eastward from the west coast (Fig. 4c). Some of this water is transported through the bottom layer back toward the bay mouth (Fig. 4d).

Figure 5 shows the monthly mean along-sectional velocity and temperature (a, c) and across-sectional heat transport (b, d) for sections S1 (a, b) and S2 (c, d), respectively, for the no-wind experiment. At the bay mouth, the currents flow eastward and are relatively stronger in the top layer and along the west coast (Fig. 5a). At the same time, cool open-ocean water is transported into the bay from the top layer and flows out from the bottom layer (Fig. 5b). In the central bay area, strong eastward currents form strong downwelling along the east coast, suppressing the isotherm downward, while isotherm levels along the west coast increase (Fig. 5c). Heat is transported to the bay head from the central bay area and then transported out of the bay head along the east and west coasts (Fig. 5d).

3.2 Effects of southerly wind

Japan Meteorological Agency and Japan Oceanographic Data Center wind observation data for the central east coast of the bay (black triangle in Fig. 1) for July were collected. Figure 6 presents the monthly mean amplitude of the southerly (black) and easterly (blue) wind components for July from 1979 to 1997. Over Tokyo Bay, southerly winds dominated, with speeds of approximately 3 to 4 m/s. To examine the effects of southerly winds on heat transport processes and the water

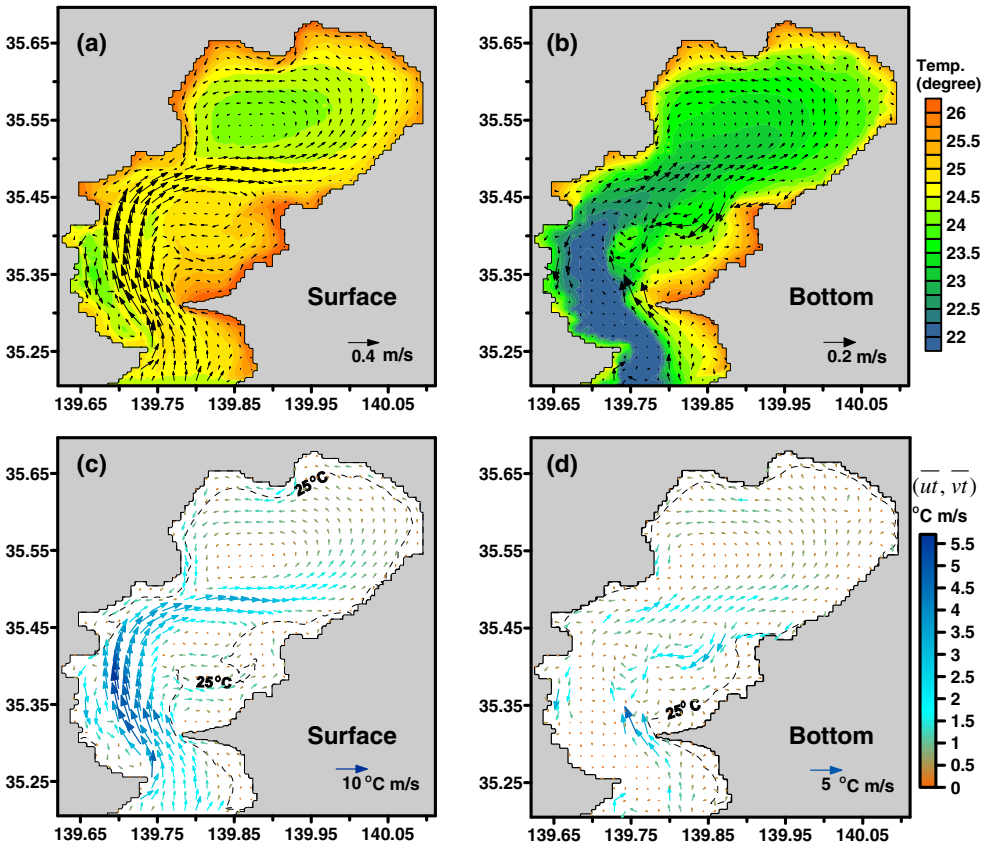

Fig. 4 (**a**, **b**) Monthly mean currents (vectors) and water temperatures (*shaded*) in surface (left) and bottom (right) layers, respectively, for the no-wind experiment. (**c**, **d**) Monthly mean heat transport in surface (left) and bottom (right) layers, respectively, in which the vectors denote the direction and color shading denotes the strength. The *dashed lines* denote the 25 °C isotherm. Note that different reference vectors are used for the bottom layer

temperature distribution, the model was executed with the 3 m/s southerly winds for July, and the results were compared with the no-wind experimental results.

Figure 7 presents the differences in the monthly mean current, temperature (a, b), and strength of heat transport (c, d) between the 3 m/s southerly wind and no-wind experimental

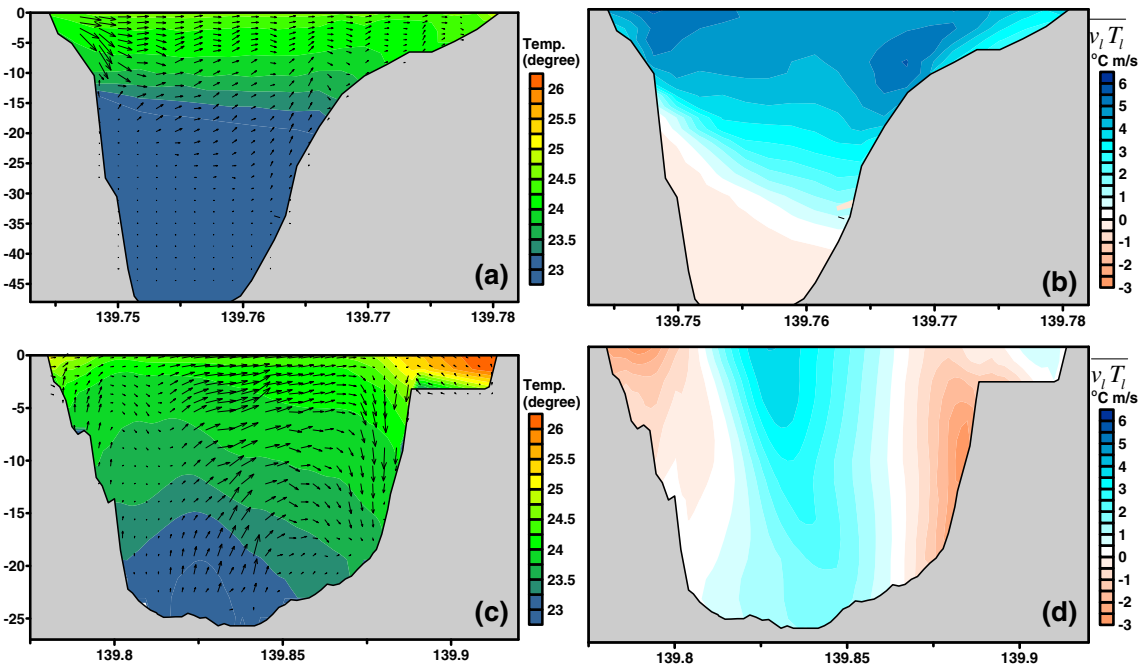

Fig. 5 Monthly mean sectional velocity and temperature (**a**, **c**) and cross-sectional heat transport (**b**, **d**) along sections S1 (**a**, **b**) and S2 (**c**, **d**), respectively, for the no-wind experiment. Note that northward transport is positive

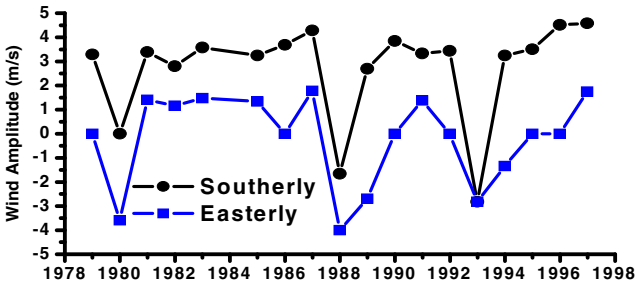

Fig. 6 Year-to-year mean wind amplitude (*black*, southward component; *blue*, eastward component) for July from 1979 to 1997 at the wind observation station (*black triangle* in Fig. 1)

results in the surface (a, c) and bottom (b, d) layers. The southerly winds intensify the northward and eastward currents in the bay, particularly along the west and east coasts of the bay head area (Fig. 7a). Consequently, in the surface layer, eastward and northward heat transport increases at the bay mouth, in the central bay area, and along the east coast, while southward heat transport along the west coast declines considerably (Fig. 7c). Consequently, more cool water flows into the bay and reaches the eastern section of the bay head area; along the west coast of the bay head, southward warm water transport declines. Thus, the water temperature decreases in most areas of the bay but increases in the western section of the bay head (Fig. 7a). Similarly, in the bottom layer, while the strength of heat transport changes little (Fig. 7d), the water temperature along the west coast of the bay head increases because warm water is forced to accumulate. In addition, along the southwest coast, both surface heat transport and water temperature decrease significantly (Fig. 7a, c). These decreases are related to the decline in clockwise circulation and the formation of upwelling in that area.

Figure 8 presents the differences in the monthly mean along-sectional temperature (a, c) and cross-sectional heat transport (b, d) between the 3 m/s southerly wind and no-wind experimental results for sections S1 (a, b) and S2 (c, d). Wind has a little influence on temperature and heat transport at the bay mouth (Fig. 8a, b). However, in the central bay area, northward heat transport increases in the top layer, causing a decline in the surface water temperature. Southward heat transport is suppressed, thereby increasing the temperature close to the west coast, particularly in the sub-surface layer (Fig. 8b, d).

3.3 Effects of northerly wind

Northerly winds occasionally prevail over Tokyo Bay with an amplitude of approximately 2.0~3.0 m/s (years 1988 and 1993 in Fig. 6). To examine the effects of northerly winds

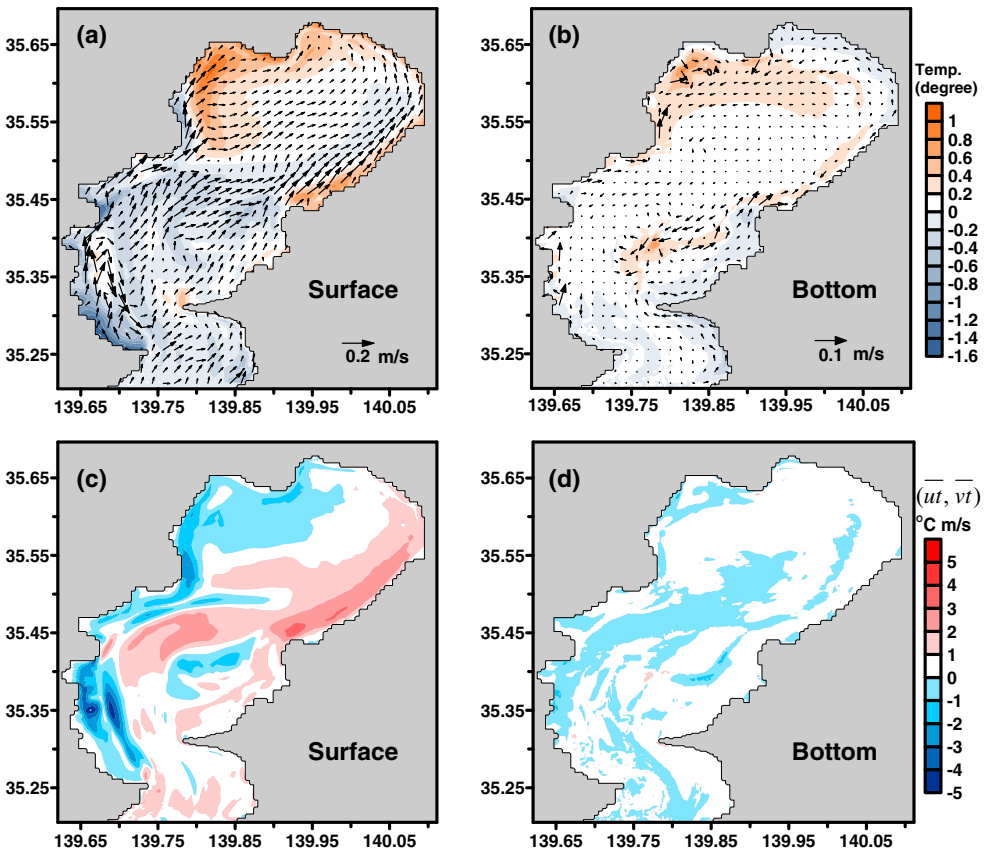

Fig. 7 Differences in monthly mean currents and temperatures (**a**, **b**) and heat-transport strengths (**c**, **d**) between the 3 m/s southerly wind and no-wind experimental results in surface (**a**, **c**) and bottom (**b**, **d**) layers. Note that different reference vectors are used for the bottom layer

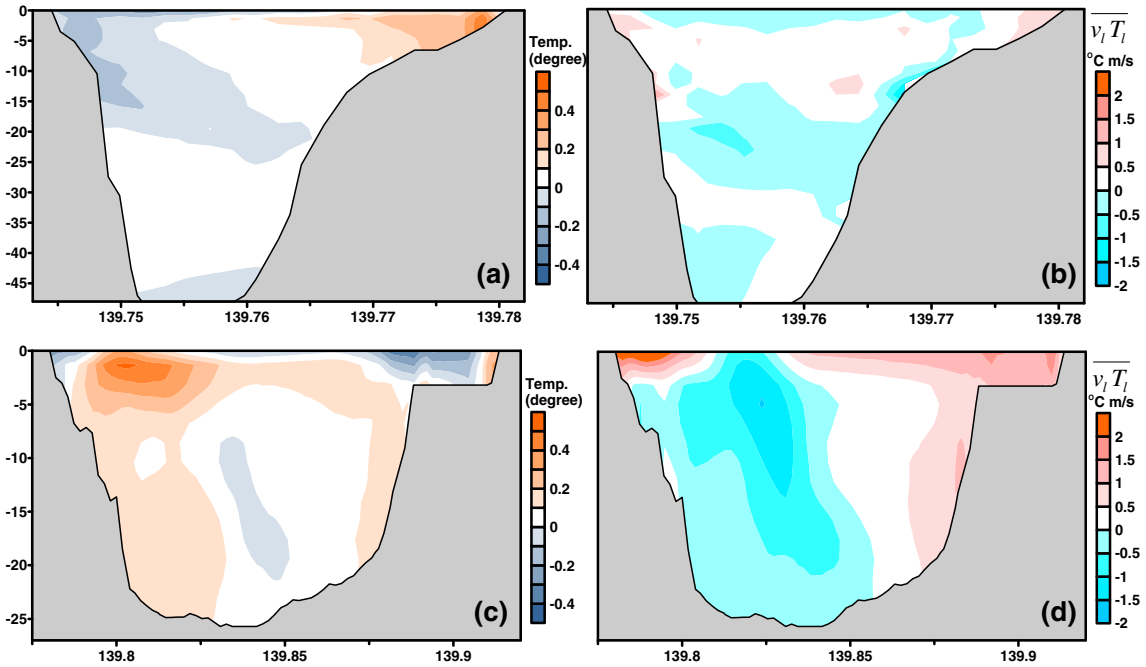

Fig. 8 Differences in monthly mean sectional temperature (**a**, **c**) and cross-sectional heat transport strengths (**b**, **d**) between the 3 m/s southerly wind and no-wind experimental results along sections S1 (**a**, **b**) and S2 (**c**, **d**)

Fig. 9 Differences in monthly mean currents and temperatures (**a**, **b**) and heat-transport strengths (**c**, **d**) between the 3 m/s northerly wind and no-wind experimental results in surface (**a**, **c**) and bottom (**b**, **d**) layers. Note that different reference vectors are used for the bottom layer

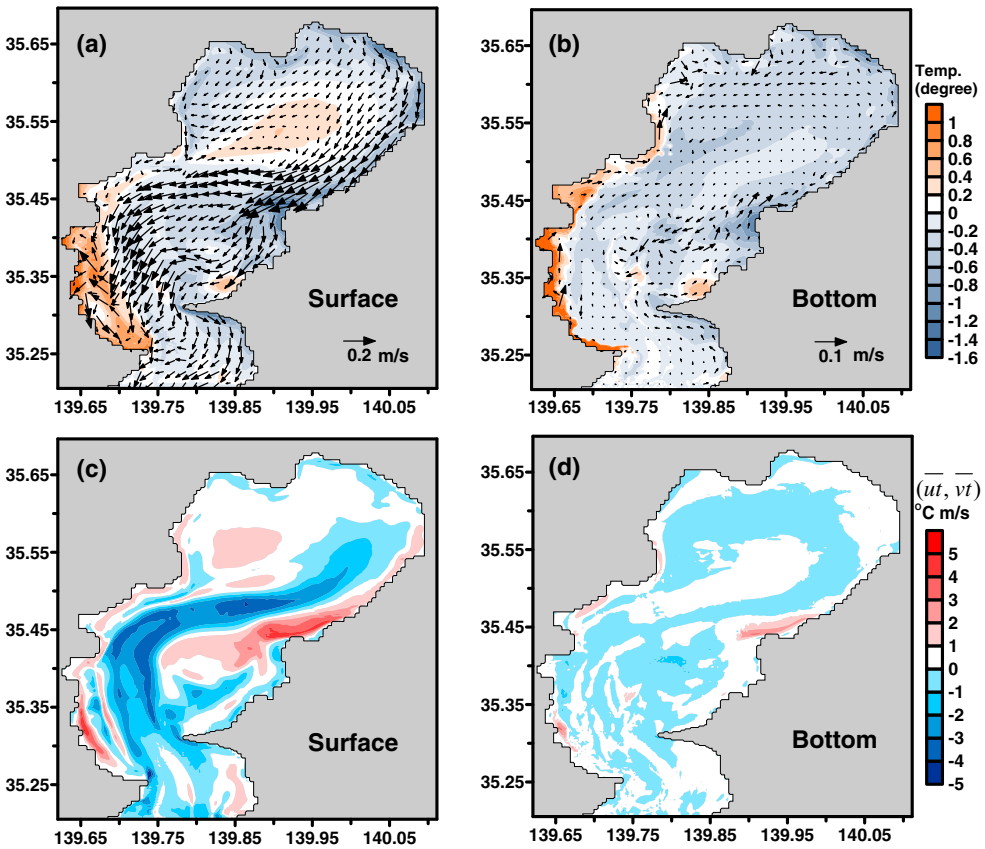

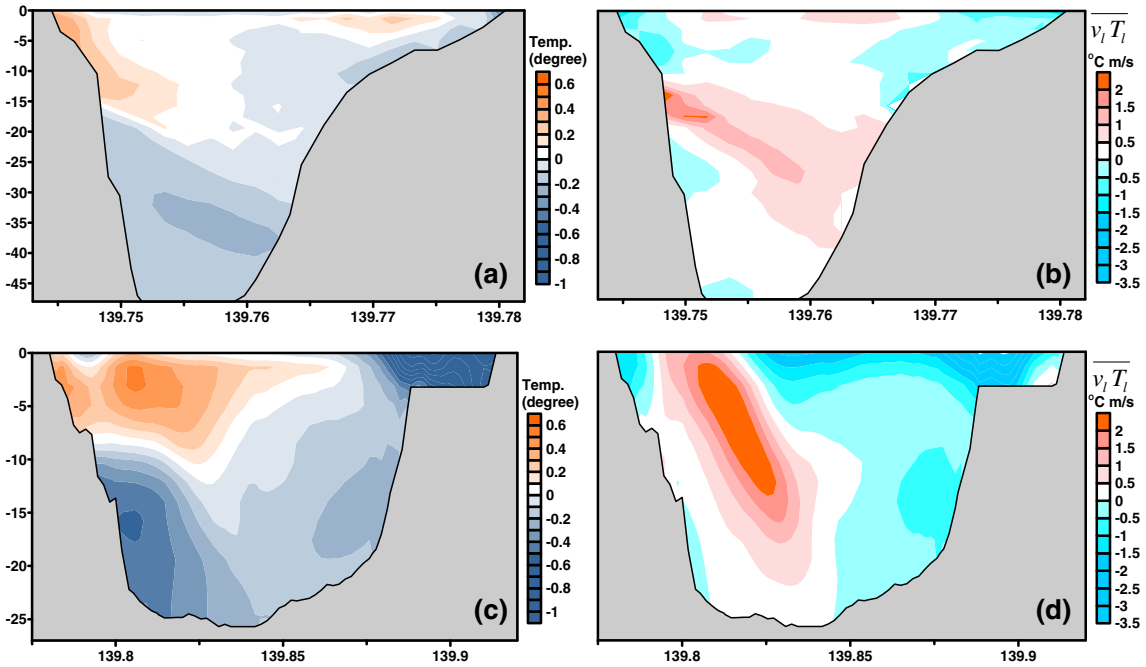

Fig. 10 Differences in monthly mean sectional temperatures (**a**, **c**) and cross-sectional heat transport strengths (**b**, **d**) between the 3 m/s northerly wind and no-wind experimental results along sections S1 (**a**, **b**) and S2 (**c**, **d**)

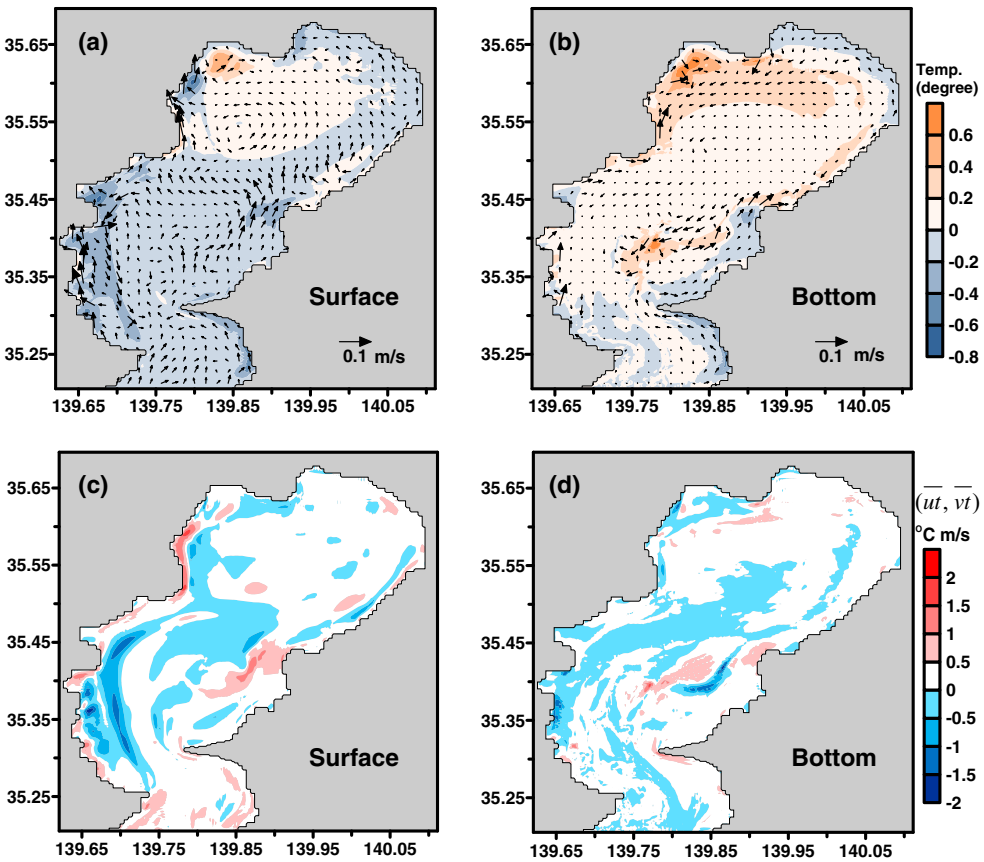

Fig. 11 Differences in monthly mean currents and temperatures (**a**, **b**) and heat-transport strengths (**c**, **d**) between the 3 and 4 m/s southerly wind experimental results in surface (**a**, **c**) and bottom (**b**, **d**) layers. Note that different reference vectors are used for the bottom layer

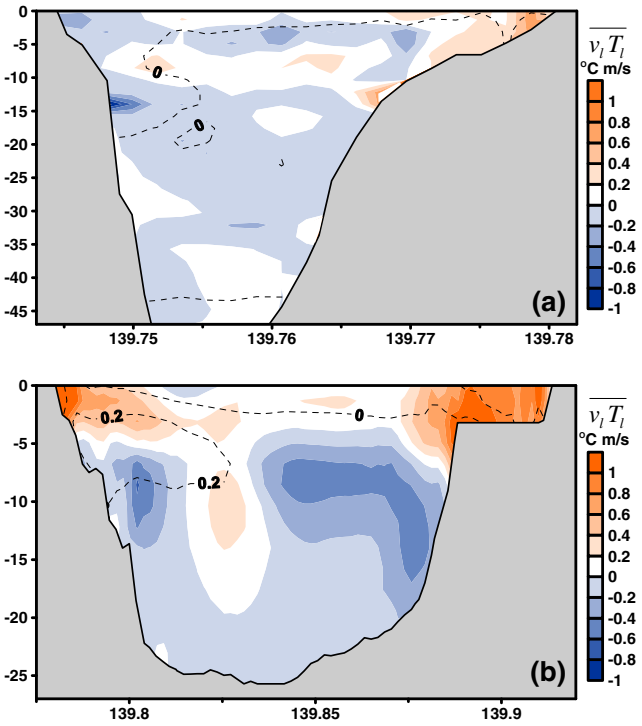

Fig. 12 Differences in monthly mean temperatures (contours in degrees) and cross-sectional heat transport strengths (*shaded*) between the 3 and 4 m/s southerly wind experimental results along sections S1 (**a**) and S2 (**b**), respectively. Note that northward transport is positive

on heat transport and the water-temperature distribution, the model was conducted under 3 m/s northerly wind conditions for July, and the results were compared with the no-wind experimental results.

Figure 9 presents the differences in the monthly mean currents and temperature (a, b) and strength of heat transport (c, d) between the 3 m/s northerly wind and no-wind experimental results for the surface (a, c) and bottom (b, d) layers. In the surface layer, northerly winds drive currents flows southwestward, considerably weakening southward heat transport in the bay while strengthening northward heat transport along the west coast (Fig. 9a, c). In this case, warm bay water is transported along the west coast and accumulates near the southwest coast, increasing the water temperature there in the both surface and bottom layers (Fig. 9a, b). Northerly winds have little influence on the heat transport at the bottom (Fig. 9d).

Figure 10 presents the differences in the monthly mean along-sectional temperature (a, c) and cross-sectional heat transport (b, d) between the 3 m/s northerly wind and no-wind experimental results for sections S1 (a, b) and S2 (c, d). When northerly winds prevail, the water temperature decreases along the east coast but increases in the subsurface layer along the west coast (Fig. 10a, c). At the bay mouth, southward heat transport declines in the surface layer but increases in the middle layer as a result of the compensatory mechanism (Fig. 10b). In the central bay area, southward heat transport along the east coast declines but strengthens near the west coast, thereby confining warm water to this area (Fig. 10b, d).

4 Effect of wind on the long-term trend of water temperature in Tokyo Bay

The modeling results demonstrated that the heat transport processes and consequent distribution of water temperature in Tokyo Bay are significantly influenced by wind forcing. Since wind is a critical factor in determining the water temperature distribution, does it affect the long-term trend of water temperature in Tokyo Bay? According to the wind observations presented in Fig. 6, from year 1979 to 1997, the wind field over Tokyo Bay was mainly dominated by southerly wind, whereas in 1988 and 1993 northerly winds prevailed. These weather conditions in July have been reported to be abnormally cool (http://www.data.jma.go.jp/gmd/cpd/db/longfcst/kikohyo_monthly.html). In this study, we focus on the typical summer weather condition and only the southerly wind trend is taken into account. Linear regression analysis provides a trend line for the southerly wind of $\hat{W}=0.08t-170.4$, where $\hat{W}$ denotes the wind speed. The linear correlation coefficient for this regression is approximately 0.5. Using a two-sided hypothesis test, we can obtain the probability to deny this linear trend (p value), which is approximately equal to 0.05. Therefore, from 1979 to 1997, the southerly wind has a trend of approximately 0.08 m/s/year at a 95 % confidence level. Thus, the southerly winds speed over Tokyo Bay increased by more than 1 m/s from 1979 to 1997. To determine the heat transport and water temperature distribution responses to this intensified southerly wind, we conducted another experiment under the 4 m/s southerly wind condition.

Figure 11 presents the differences in the monthly mean currents and temperature (a, b) and strength of heat transport (c, d) between the 3 and 4 m/s southerly wind experimental results in the surface (a, c) and bottom (b, d) layers. The differences in temperature between these two experimental results (Fig. 11a, c) follow the long-term water temperature trends presented by Ando et al. (2003); that is, in the surface layer, the central bay and bay mouth water temperatures clearly decreases, while in the bay head area, the temperature decreases little and even increases in the northwest corner. In the bottom layer, water temperature clearly increases at the bay head and in the east region of the central bay area. The variations in the strength of the heat transport (Fig. 11c, d) suggest that the intensified southerly wind alters heat content in different areas of the bay and redistributes water temperatures.

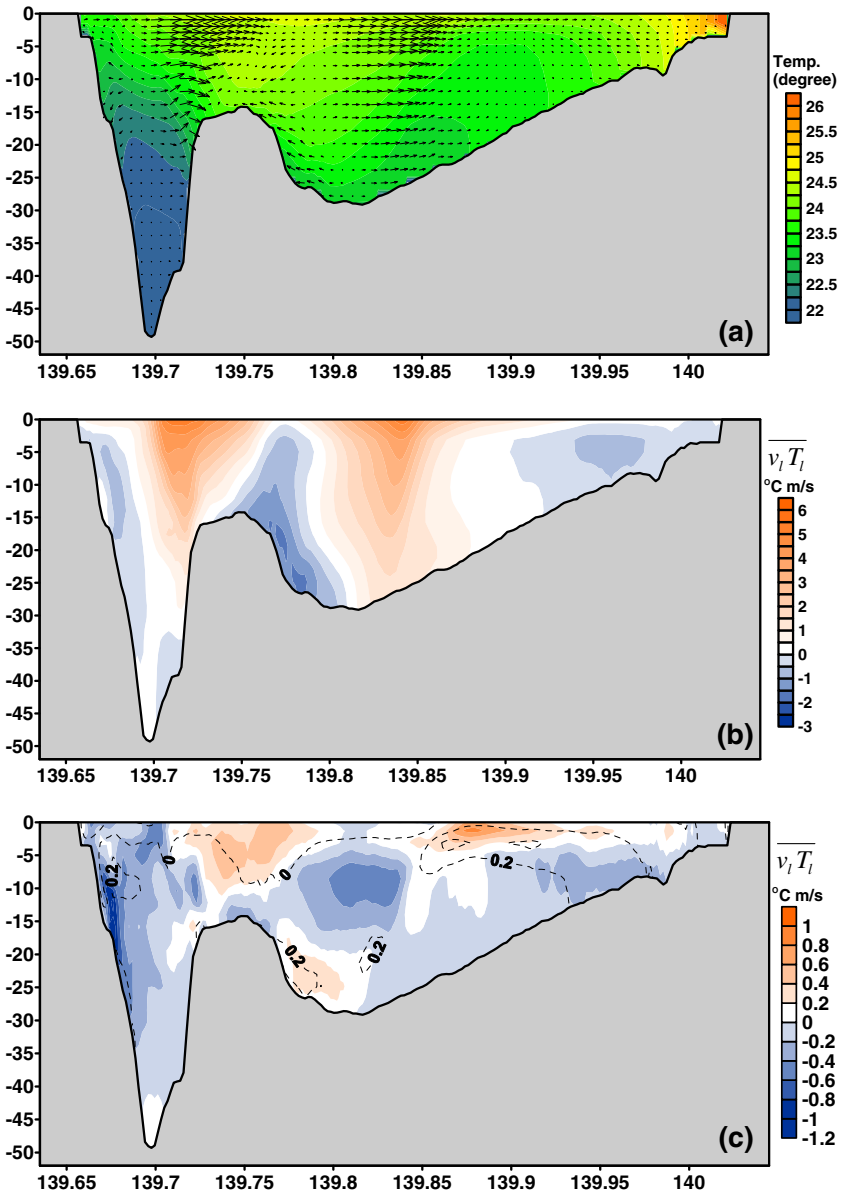

Fig. 13 Monthly mean sectional velocity and temperatures (**a**) and along-sectional heat transport strength (**b**) along section S3 for the 3 m/s southerly wind experiment and differences in monthly mean temperatures (contours in degree) and along-sectional heat transport strength (*shaded*) between the 3 and 4 m/s southerly wind experimental results along section S3 (**c**). Note that northward transport is positive

The regional heat content was calculated for the two cases using the following equation:

$$Q = \rho c_{\mathrm{p}} \iiint T \, dxdydz \tag{7}$$

in which Q is the total heat content for the entire region and c_{p} is the specific heat for water, approximately 4.2×10^{3} J/kg^{-1}/°C. For the entire bay, when the southerly winds increase from 3 to 4 m/s, the total heat content Q_{tot} increases from approximately 4.432×10^{6} to 4.45×10^{6}, and their difference ΔQ_{tot} is approximately 1.8×10^{4}. The heat content in the bay head area Q_{head} was also calculated. When the southerly winds increase, Q_{head} increases from approximately 1.89×10^{6} to 1.905×10^{6}, and their difference ΔQ_{head} is about 1.5×10^{4}, which is approximately equal to ΔQ_{tot}. Therefore, the increase of total heat content induced by intensified southerly winds mainly comes from the bay head area.

Based on the heat balance for Tokyo, the surface Q_{air} and lateral open boundary Q_{lateral} heat fluxes are the only two factors that affect the time rate change of total heat content, that is

$$\begin{aligned}\frac{\partial Q}{\partial t} &= Q_{\mathrm{air}} + Q_{\mathrm{lateral}} \\ &= \rho c_p \left(\iint_{\mathrm{surface}} q_{\mathrm{air}} dxdy + \iint_{\mathrm{lateral}} v_{\mathrm{l}} T_{\mathrm{l}} dxdz \right)\end{aligned} \tag{8}$$

in which q_{air} is the surface heat flux and v_{l} and T_{l} are the velocity and temperature at the transect of the lateral open boundary (section S1 for the entire bay area and section S2 for the bay head area), respectively. In the above equation, Q_{air}

is related to seasonal variations in surface heat flux and is small relative to the heat flux at the bay mouth Q_{mouth}. Consequently, the heat content of the entire bay or bay head area is dominated by net heat transport v_1T_1 across the lateral open boundary.

Figure 12 presents the differences in the monthly mean temperature (contours; in degree) and cross-sectional heat transport (shaded) between the 3 and 4 m/s southerly wind experimental results for sections S1 (a) and S2 (b). At the bay mouth, intensified southerly winds have little influence on water temperature and heat transport (Fig. 12a). However, in the central bay area, intensified southerly winds greatly affect water temperature and heat transport (Fig. 12b). Along the west and east coastal regions, although water temperature decreases, northward currents grow stronger after southerly winds intensify, increasing heat input in the surface layer along both coasts (Fig. 12b). While beneath the surface layer, the water temperature slightly increases on along the west coast, and the heat output also increases. Consequently, the net heat input along section S2 increases.

To further illustrate this phenomenon, Fig. 13 presents the monthly mean sectional velocity and temperature (a) and sectional heat transport (b) for section S3 under the 3 m/s southerly wind condition. The differences in the monthly mean temperature (contours in degree) and sectional heat transport (shaded) between the 3 and 4 m/s southerly wind experimental results for section S3 are also shown (Fig. 13c). Under southerly wind conditions, the currents along section S3 flow northward, inducing upwelling along the southwest coast and downwelling along the northeast coast with a rise and fall of isotherms, respectively. In the bottom layer, there is a return flow north of Futtsu Cape (Fig. 13a). The water temperature exhibits a strong stratified structure near the bay mouth but is less stratified and becomes fully mixed in the central bay and bay head areas (Fig. 13a). Following these currents and water temperature distributions, heat transport along section S3 exhibits strong northward heat transport in the central bay, while to the north of Futtsu Cape, southward heat transport occurs as a result of counterflows (Fig. 13b). In the bay head area, the heat is transported northward at surface. Upon reaching the north coast, the currents turn to southward (Fig. 13a), producing southward heat transport beneath the surface layer (Fig. 13b). When southerly winds intensify, upwelling is strengthened in the surface layer, leading to stronger northward heat transport and lower water temperature near the bay mouth (Fig. 13c). In the bay head area, northward heat transport also strengthens at the surface. Concurrently in the bottom layer, although the southward heat transport also increases, it cannot compensate for the increase in northward heat transport, thus causing the water temperature increases there (Fig. 13c).

5 Conclusion

In this study, the effect of wind on long-term summer water temperature trends in Tokyo Bay was studied using several numerical experiments. The modeling results indicate that winds have a pronounced influence on the heat transport as well as water temperature distribution in Tokyo Bay: (1) when southerly winds prevail, northward cool-water transport is intensified while southward warm-water transport is suppressed, thereby decreasing the water temperature in the central bay area but increasing the water temperature at the bay head; (2) northerly winds have the opposite effect, causing the water temperature to decrease in coastal bay head areas but increase along the southwest coast.

Intensified southerly winds may have affected long-term summer water temperature trends from 1976 to 1997, as reported by Ando et al. (2003). The comparison of the numerical experiments under the 3 and 4 m/s wind conditions reveals that winds influence the water temperature trend by (1) enhancing upwelling along the southwest coast and more effectively transporting upwelled water northward, decreasing water temperatures at the bay mouth and central bay areas, and (2) suppressing southward heat transport from the bay head, increasing water temperature there as well as in the bottom layer through downwelling in the north region of the bay head.

Although the present modeling results indicate that intensified southerly winds significantly affect water temperature trends in Tokyo Bay, several other influencing factors must also be considered, such as air temperature, heat input from rivers, sewage, and plants. The effects of these variables on long-term water temperature trends should be investigated in future studies.

Acknowledgments This study was supported by the Research Program on Climate Change Adaptatoin (RECCA) led by the Ministry of Education, Culture, Sports, Science and Technology of Japan. The numerical simulations presented in this study were conducted on the Earth Simulator II supercomputer based at the Japan Agency for Marine-Earth Science and Technology. Two anonymous reviewers are thanked for their valuable and constructive comments and suggestions.

References

Ando H, Kashiwagi N, Ninomiya K, Ogura H, Yamazaki M (2003) Long term trends of seawater temperature in Tokyo Bay. Oceanogr Jpn 12(4):407–413 (in Japanese with English abstract)

Antonov JI, Seidov D, Boyer TP, Locarnini RA, Mishonov AV, Garcia HE, Baranova OK, Zweng MM, Johnson DR (2010) World Ocean

Atlas 2009, Volume 2: Salinity. S. Levitus, Ed. NOAA Atlas NESD IS 69, U.S. Government Printing Office, Washington, D.C., 184 pp

Aoki K, Isobe A (2006) Numerical study of the summer temperature decrease induced by the enhancement of estuarine circulation in Fukuoka Bay. J Oceanogr 62:207–217

Chang Y-L, Oey L-Y (2010) Eddy and wind-forced heat transports in the Gulf of Mexico. J Phys Oceanogr 40:2728–2742

Fairall CW, Bradley EF, Hare JE, Grachev AA, Edson JB (2003) Bulk parameterization of air-sea fluxes: Updates and verification for the COARE algorithm. J Clim 16:571–591

Guo X, Yanagi T (1996) Seasonal variation of residual current in Tokyo Bay, Japan—Diagnostic numerical experiments. J Oceanogr 52: 597–616

Hinata H, Nadaoka K, Yagi H, Tabuchi H, Yoshioka T (2001) Currents and material transport in Tokyo Bay due to coastal warm water intrusion induced by the Kuroshio fluctuation in stratified condition. J Hydraul Coast Environ Eng 684:93–111 (in Japanese with English abstract)

Kalnay E, Kanamitsu M, Kistler R, Collins W, Deaven D, Gandin L, Iredell M, Saha S, White G, Woollen J, Zhu Y, Leetmaa A, Reynolds R, Chelliah M, Ebisuzaki W, Higgins W, Janowiak J, Mo KC, Ropelewski C, Wang J, Jenne R, Joseph D (1996) The NCEP/NCAR 40-Year reanalysis project. Bull Amer Meteor Soc 77:437–471

Locarnini RA, Mishonov AV, Antonov JI, Boyer TP, Garcia HE, Baranova OK, Zweng MM, Johnson DR (2010) World Ocean Atlas 2009, Volume 1: Temperature. S. Levitus, Ed. NOAA Atlas NESDIS 68, U.S. Government Printing Office, Washington, D.C., 184 pp

Magome S, Goda Y, Kobayashi R, Irie M, Imai N, Gomi H, Shirai K, Suzuki N (2012) Effects of wind stress and density stratification and freshwater inflow on the water exchange in Tokyo Bay. J JSCE, B2 (Coast Eng) 68(2):956–960 (in Japanese with English Abstract)

Marshall J, Hill C, Perelman L, Adcroft A (1997a) Hydrostatic, quasi-hydrostatic, and nonhydrostatic ocean modeling. J Geophys Res 102(C3):5733–5752

Marshall J, Adcroft A, Hill C, Perelman L, Heisey C (1997b) A finite-volume, incompressible Navier Stokes model for studies of the ocean on parallel computer. J Geophys Res 102(C3):5753–5766

Mellor GL, Yamada T (1982) Development of a turbulent closure model for geophysical fluid problems. Rev Geophys Space Phys 20(4): 851–875

Nakayama K, Shintani T, Shimizu K, Okada T, Hinata H, Komai K (2014) Horizontal and residual circulation driven by wind stress curl in Tokyo Bay. J Geophys Res Oceans. doi:10.1002/2013JC009396

Nixon SW, Granger S, Buckley BA, Lamont M, Rowell B (2004) A one hundred and seventeen year coastal water temperature record from Woods Hole, Massachusetts. Estuaries 27(3):397–404

Nomura H (1996) Interaction between the inlet and the open ocean: a biological approach using time-series record of meso- and macrozooplankton community structure in Tokyo Bay as an index of water exchange. Bull Coast Oceanogr 34(1):25–35 (in Japanese with English abstract)

Oda R, Kanda M (2009) Observed sea surface temperature of Tokyo Bay and its impact on urban air temperature. J Appl Meteorol Climatol 48:2054–2068

Onishi Y (1975) Development of the current induced by the topographic heat accumulation (I) — the case of the axisymmetric basin. J Oceanogr Soc Japan 31:243–254

Preston BL (2004) Observed winter warming of the Chesapeake Bay estuary (1949-2002): Implications for ecosystem management. Environ Assess. doi:10.1007/s00267-004-0159x

Shearman RK, Lentz SJ (2010) Long-term sea surface temperature variability along the U.S. east coast. J Phys Oceanogr 40:1004–1017

Smagorinsky J (1963) General circulation experiments with the primitive equations- I. the basic experiment. Mon Weather Rev 91(3):99–165

Suzuki T, Matsuyama M (2000) Numerical experiments on stratified wind-induced circulation in Tokyo Bay, Japan. Estuar Coast Shelf Sci 50:17–25

Tabeta S, Fujino M (1996) Comparison of simulation results and field data on currents and density in Tokyo Bay. J Mar Sci Technol 1:94–104

Unoki S, Okazaki M, Nagashima H (1980) The circulation and oceanic condition of Tokyo Bay. Technical Report of Physical Oceanography Laboratory, the Institute of Physical and Chemical Research, No. 4, March, 1980 (in Japanese)

Yagi H, Ishida H, Yamaguchi H, Kinouchi T, Toida S, Ishii M (2004) Characteristic of long-term changes in temperature in Tokyo Bay and surrounding area. Proc Coast Eng JSCE 51:1236–1240 (in Japanese)

Yanagi T (2008) Great water temperature changes of 1.5 °C per decade in Tokyo Bay, Japan—its causes and consequences. J Disaster Res 3(2):113–114